Aerosol and Air Quality Research, 18: 2618–2632, 2018

ISSN: 1680-8584 print / 2071-1409 online
doi: 10.4209/aaqr.2018.03.0105

Size Distribution of Ultrafine Particles Generated from Residential Fixed-bed Coal Combustion in a Typical Brazier

Daniel M. Masekameni[1,2*], Derk Brouwer[1], Tafadzwa Makonese[3], Isaac T. Rampedi[2], Mary Gulumian[4]

[1] *Occupational Health Division, School of Public Health, University of the Witwatersrand, Parktown, Johannesburg 2193, South Africa*
[2] *Department of Geography, Environmental Management and Energy Studies, University of Johannesburg, Johannesburg 2006, South Africa*
[3] *SeTAR Centre, Faculty of Engineering and the Built Environment, University of Johannesburg, Johannesburg 2006, South Africa*
[4] *National Institute for Occupational Health, National Health Laboratory Services, Braamfontein, Johannesburg 2000, South Africa*

ABSTRACT

Ultrafine particles (with a small mean diameter) released from domestic coal combustion are an important parameter to consider in air pollution, as they affect air quality and human health. It has been suggested that poor combustion conditions release particles of different sizes enriched with health-damaging chemicals, such as polycyclic aromatic hydrocarbons. Furthermore, both smouldering and highly efficient combustion conditions release particles, which are often carcinogenic. Information on the particle size distribution (PSD) of char or soot emitted from fixed-bed domestic coal combustion is limited, with many studies reporting on wood combustion. This study investigated the influence of coal combustion phases (ignition, flaming, and coking) on the particle number concentration and size distribution of ultrafine particles. D-grade bituminous coal was crushed to a particle diameter (Ø) of 40–60 mm and combusted in a laboratory designed coal brazier (*Imbaula*) during experimental investigations of the particle size distribution normalised to the particle number concentration against the particle diameter. Experiments were carried out using the reduced smoke top-lit updraft method, colloquially known as the *Basa njengo Magogo* (BnM) method. The tests were carried out in a laboratory-controlled environment. Particulate matter was monitored using a NanoScan Scanning Mobility Particle Sizer (SMPS). Particles from the top-lit updraft (TLUD) showed an ultrafine geometric mean diameter centred at approximately 109 ± 18.4 nm for the ignition phase, 54.9 ± 5.9 nm for the pyrolysis/flaming phase, and 31.1 ± 5.1 nm for the coking phase. The particle mode diameter rapidly increased during the ignition phase (145 nm) and gradually decreased during the flaming phase (35 nm) and the coking phase (31 nm). This study shows that during smouldering combustion conditions (ignition), the particle diameter increases, whereas it decreases as the temperature increases. This information is essential for estimating particle deposition in the lungs and the associated health risks.

***Keywords*:** Particulate matter; Brazier; Scanning mobility particle sizer.

INTRODUCTION

Over half of the global population continue to depend on solid-fuels for domestic cooking and heating, with the majority found in developing countries (Bonjour *et al.*, 2013; International Energy Agency, 2015). Household solid-fuel burning releases copious amounts of particulate matter mostly associated with increased health and environmental risks (Smith and Peel, 2010; Zhang *et al.*, 2012). Small-scale combustion processes such as biomass and coal-burning are major sources of fine particulate matter leading to high levels of household air pollution (HAP). As such, studies on poor indoor air quality have received renewed interest due to associated health consequences (Dockery *et al.*, 1993; Andreae and Merlet, 2001; Cincinelli and Martellini, 2017). Domestic solid-fuel burning using inefficient cookstoves has been identified as a significant source of poor air quality in human settlements in both developed and developing countries (Dockery *et al.*, 1993; GACC, 2009; Smith and Peel, 2010).

* Corresponding author.
Tel.: +2711 717 2355
E-mail address: danielmasekameni@gmail.com

Most studies have focused on large-scale solid-fuel combustion systems including power plants and large boilers as significant sources of ambient particulate matter concentration (Gladney, 1974; Gladney, 1976; McElroy *et al.*, 1982; Morawska *et al.*, 2008). Efforts to separate large-scale combustion particles from residential solid-fuel burning suggested that particles from the industrial operation are more than 100 nm in diameter but can grow during the accumulation mode to 1000 nm (Kumar *et al.*, 2011). Particulate matter (PM) emissions from residential coal burning are estimated to be at a size range of lower than 100 nm. However, the particle diameter can grow to 300 nm during accumulation mode (Morawska *et al.*, 2008). This differentiation based on size fraction can be used in source apportionment exercises (Naeher *et al.*, 2007).

Extensive epidemiological studies pointed out that exposure to particulate matter (PM) below 2.5 μm either on a short or long-term basis lead to the development of cardiovascular and respiratory diseases, which reduces life expectancy (Dockery *et al.*, 1993). It is estimated that, globally, household air pollution is responsible for 4.3 million aggravated mortalities (Gordon *et al.*, 2014; Forouzanfar *et al.*, 2015). Several studies have shown that solid-fuel combustion is a significant contributor to increased premature mortalities (Smith *et al.*, 1994; Lim *et al.*, 2012). A study conducted by the European Environmental Agency between 2010 and 2012 revealed that inhalation of combustion particles resulted in 400,000 premature deaths throughout Europe (Rainey *et al.*, 2016). A study carried out in Mpumalanga, South Africa, in 2012 indicated 8% hospital admissions and 9% mortalities per annum due to combustion particles. In the City of Tshwane, South Africa, 20–25% hospital admissions and respiratory-related mortalities per annum were attributed to inhaling domestic coal combustion particles (Scorgie, 2012). Furthermore, smoke emissions from combustion activities were responsible for 4.3% and 6% infant mortality rates per annum in Mpumalanga Province and the City of Tshwane, respectively (Stats SA, 2010).

Globally, it is envisaged that there is a need to introduce clean energy alternatives as a mechanism to reduce dependence on solid-fuels for domestic cooking, heating and lighting (International Energy Agency, 2015). Furthermore, other studies suggest that reducing emissions of PM will minimize incidences of air pollution health risks and premature mortalities (GACC, 2009; ISO IWA, 2012; WHO, 2014). The dissemination of improved cookstoves is seen as a viable option to reducing exposure to noxious pollutants from household energy uses (Smith *et al.*, 2007). Successful cookstove dissemination programmes have been reported in Asia and Africa (Smith *et al.*, 2004). Literature suggests that with improved combustion conditions, there is a possibility of reduced particle emissions (Le Roux *et al.*, 2004; Zhang and Smith, 2007; Makonese *et al.*, 2015). However, recent studies have shown that enhanced combustion conditions release fine particles (Kumar *et al.*, 2010; Zhang *et al.*, 2012; Tiwari *et al.*, 2013).

For decades, emissions of particulate matter by mass concentrations (given in unit mg m^{-3}) were widely used to estimate the potential harm of PM to the human population (Jian and Bell, 2008). However, in a separate study conducted on emissions from diesel combustion, reporting exposure using mass-based emissions was criticized. The authors reported that particles of larger diameter presented minimum harm to humans relative to ultrafine particles (Kittelson, 1998; Fernandez *et al.*, 2003; Bølling *et al.*, 2009). Ultrafine particles contribute less to the PM mass, but they present severe human health effects due to their large surface area and higher deposition efficiency in the small airways and alveoli of the lungs, subsequently translocate to other vital organs through the bloodstream (Oberdörster *et al.*, 2005; Tranfield and Walker, 2012). Due to the health consequences posed by solid-fuels, there has been considerable effort to characterise coal combustion products dating back to the 1970s. Submicron aerosols from coal combustion have been found to have a stronger impact on human health as they are enriched with toxic elements (Kauppinen and Pakkanen, 1990; Smith *et al.*, 2009). In addition to the toxic substances contained in coal combustion particles, is the ability of the submicron particles to remain suspended in the air for a prolonged duration, which increases the risk of exposure (Kauppinen and Pakkanen, 1990). In light of this, fine and ultrafine particles from domestic coal combustion are receiving increased attention in South Africa, from both the scientific community and environmental management regulators.

Domestic coal combustion in South Africa is a major source of PM emissions in both ambient and indoor environments (Ezzati *et al.*, 2000; Scorgie *et al.*, 2003; Bruce *et al.*, 2000; Barnes *et al.*, 2005, 2009). During the early 1990s, over 20 million people daily combusted coal as their primary source of energy for domestic cooking, heating and water boiling (Terblanche *et al.*, 1994; Annegarn and Sithole, 1997). The government of South Africa introduced mass electrification program aiming at delivering access to poor households to reduce dependence on coal and other solid-fuels (DME, 2004). By the end of 2006, over 73% of human settlements were connected to the electricity grid (DME, 2006). However, half of the people continued to rely on coal and wood for domestic cooking (Balmer, 2007). Other surveys indicated a sustained reduction in coal and wood dependence over the years with electricity being a significant source for cooking and heating (Statistics South Africa, 1998, 2003, 2007). To the contrary, a study conducted by Makonese *et al.* (2016) in Johannesburg's informal settlements found that over 90% of the surveyed households relied on coal for cooking and space heating. Moreover, Kasangana *et al.* (2017) found that over 80% of households in Mpumalanga depend on wood for space heating and cooking. Location and fuel availability dictate the differences in energy use patterns. In the Highveld, reliance on coal is high while in the Lowveld, wood is the dominant fuel (Balmer, 2007).

During coal combustion, the underlying mechanisms on how particles are formed and released depend on various factors. Particles from freshly emitted soot are in the fine mode, which includes the nuclei and the accumulation mode (Anastasio and Martin, 2001). During the nucleation phase, particles are formed from the condensation of a low-

pressure vapour in the atmosphere or through atmospheric chemical reactions. These particles have a diameter of less than 100 nm (Sioutas *et al.*, 2005). After nucleation the particles undergo accumulation. In this stage, the smaller particles coagulate with other particles to form diffusion accretion chains that are 100–1000 nm long (Kumar *et al.*, 2011). Primary particles from combustion processes, often produced as soot, remain an essential factor in understanding particle transportation and deposition. It is accepted that fine particles remain airborne in the atmosphere for a longer duration, thus increasing the exposure potential. Due to their smaller diameter, combustion particles are less susceptible to gravity increasing the resident time and can travel a longer distance (Kumar *et al.*, 2010).

According to Hosseini *et al.* (2010), particle size distribution can differ as a function of the combustion phase (ignition, flaming, coking), fuel characteristics (moisture content, ash content, thermal content) and fuel types (lignite, bituminous, anthracite). Several studies have documented emissions from different coal combustion processes due to the importance of particle size on air quality, health and climate modelling (Linak *et al.*, 2002; Yi *et al.*, 2008; Xu *et al.*, 2011; Zhang *et al.*, 2015). PSDs from coal combustion have been studied for a variety of coal combustion processes including boilers (Kauppinen and Pakkanen, 1990; Linak *et al.*, 2002), power stations (Yi *et al.*, 2008), and drop tube furnaces (Xu *et al.*, 2011). However, earlier studies have shown a wide variation in PSD due to differences in the combustion conditions, as well as measurement techniques and the instruments used (Kauppinen and Pakkanen, 1990). To date, there is limited information on PSD from fixed-bed domestic coal combustion processes (Zhang *et al.*, 2015). Previous studies on residential coal combustion in South Africa have focused on the development of mass and energy specific emission factors (van Niekerk, 1997; CSIR, 2005; Makonese *et al.*, 2014).

A suite of instruments has been employed to determine PSD from coal combustion processes. These include include Nano Scanning Mobility Particle Sizer (SMPS) (Linak *et al.*, 2002), Aerodynamic Particle Sizer (APS) (Linak *et al.*, 2002), Low-Pressure Impaction (LPI) (Linak *et al.*, 2002; Kauppinen and Pakkanen, 1990), Electrical Low Pressure Impactor (ELPI) (Yi *et al.*, 2008), Dekati Low Pressure Impactor (DLPI) (Xu *et al.*, 2011), and Wide-range Particle Spectrometer (WPS) (Zhang *et al.*, 2015). This study makes use of the Nano Scanning Mobility Particle Sizer, since it has been widely used in similar studies and results are comparable. Zhang *et al.* (2012) conducted a survey of particle size distribution from burning coal under laboratory-controlled conditions using particle spectrometer (WPS, Model 1000XP, MSP Co., USA). Fine particles were emitted and had a mode of 63 nm for the flaming stage of combustion. Similar to Zhang *et al.* (2012), Tiwari *et al.* (2014) reported PSD of coal fires in the fine mode with the mean diameter of around 43 nm using a Differential Mobility Analyser (DMA) and a Condensation Particle Counter (CPC). However, in both studies, the description of the device, coal size, stove operational mode and ignition methods were not adequately provided.

It has been demonstrated in previous studies that a high air ventilation brazier ignited using top-lit updraft method (TLUD) improves the combustion condition significantly (Masekameni *et al.*, 2014) compared to igniting a poorly ventilated brazier using the bottom-lit updraft (BLUD) (Makonese *et al.*, 2015). Therefore, experiments in this study are limited to a high air ventilation brazier and the TLUD ignition method. Experimental studies to compare the PSD between the TLUD and the BLUD are recommended for future work. The present study focused on the submicron particles (11 nm–365 nm) and aimed to assess the number size distribution of particles emitted from fixed-bed coal combustion in typical braziers using the TLUD method. A suite of monitoring instruments including the NanoScan Mobility Particle Sizer (SMPS) was employed to measure the evolution of PSD from the ignition phase to the coking phase of combustion. This study reports, for the first time, detailed PSD from domestic coal combustion in braziers in use in the Highveld region of South Africa.

MATERIALS AND METHODOLOGY

Combustion Lab

Experiments were conducted at the SeTAR Centre stove testing laboratory, situated at the University of Johannesburg, Bunting Road Campus. The combustion experiments were carried out in a galvanized iron hut that houses the measuring and monitoring equipment. The flue gases from the burning fuel were exhausted through a 4 m long chimney (located in the center of the laboratory) with a diameter of 15 cm. A detailed description of the combustion facility including the sampling trains is given in Makonese *et al.* (2015). Unlike in Hosseini *et al.* (2010), the SeTAR lab was not pressurized with preconditioned ambient air to control parameters such as temperature and humidity. This can only be done if the primary goal is to capture all the entrainment through the ducting system. The SeTAR Heterogeneous stove Testing Protocol (HTP) uses a chemically mass balanced method to determining emission factors/rates—a representative sample of the exhaust is needed for this determination (Makonese, 2015).

Stove Description

In the present work, we investigated PSD using high air ventilation laboratory designed braziers, where holes were punched uniformly at the same size around the device. The design parameters of the braziers are provided in Table 1 and photograph of a high ventilation brazier is shown in Fig. 1.

Fuel and Fire Preparation

It has been reported elsewhere that coal characteristics (moisture content, ash content, thermal content) and fuel type (lignite, anthracites and bituminous) produces different PSD (Hossien *et al.*, 2010). In this study, we have used bituminous D-grade coal commonly used in the townships of South Africa, and we ensured that coal characteristics remained constant throughout the experiments. The coal used in this study was purchased from Slater coalmine in

Table 1. Stove ventilation rate characterisation.

Brazier ventilation rate	Height (mm)	Dia. (mm)	Grate height (mm)	Area of holes below grate (cm^2)	Area of holes above grate (cm^2)	Total area of holes (cm^2)
High	370	290	185 (50%)	248 (61%)	159 (39%)	407

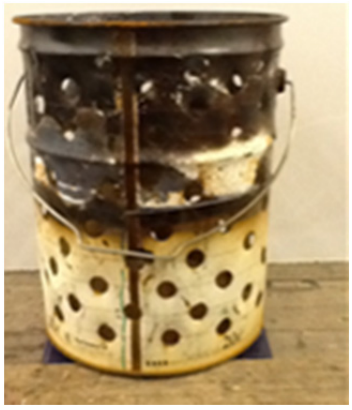

Fig. 1. Laboratory designed high ventilation stove.

the Mpumalanga Province. The fuel was stored at room temperature of 21°C in sealed containers to prevent moisture loss. The coal was homogeneously mixed using a shovel before a sample was taken for external analysis. The coal was crushed and sieved to maintain a mean size diameter of 40–60 mm. Each batch of fuel was analyzed for moisture content before the test experiments commenced. For this study, a D-grade type of bituminous coal was used in a high ventilation field *Imbaula* using the top-lit updraft method (TLUD). The fuel specifications, the high ventilation brazier, and the order of laying a top-lit updraft fire are presented in detail elsewhere (see Makonese *et al.*, 2014).

The fire was set out using government advocated ignition method, but less favored top-lit updraft (TLUD) method, colloquially known as *Basa njengo Magogo* (meaning "make fire like a granny"). The stove was set using ~35 g of paper, ~400 g of wood kindling and ~4000 g of coal. The same mass of wood and paper was used for the three tests. During the TLUD ignition method, the fuel arrangement in the brazier entailed placing 2500 g of coal on the grate, followed by the paper (35 g), wood (400 g), and the remaining 1500 g of coal on top as in Fig. 2. The entire stove was placed on a heat shield located on the platform of the mass balance. The use of a heat shield was to protect the mass balance from overheating and fire damage.

Fuel Analysis and Moisture Content

The D-grade bituminous coal used in this study was sent to a South African National Accreditation System (SANAS) accredited laboratory for analyses before the experiments commenced. The fuels were characterised for proximate analysis (moisture, ash, volatile organic compounds, fixed carbon) and ultimate analysis (C, H, S, N, O and mineral elements) given in percentage weight, analysed on an air-dried basis (wt.%, adb).

The coal moisture content (MC) was further verified before testing as different MC values can affect the combustion characteristics of the stove. A small representative sample (~100 g) was weighed on a calibrated scale with a 0.1 g resolution and then dried in an oven at 100°C for 48 hours, assuming that the 48-hour duration is sufficient for the coal to achieve steady moisture equilibrium. The sample was then taken out and reweighed. The exercise was repeated every three hours to check that the fuel had attained dry mass (Makonese *et al.*, 2017). The percentage moisture content was calculated using Eq. (1):

$$M = \frac{M_{wet} - M_{dry}}{M_{wet}} \times 100 \quad (1)$$

where M_{wet} is the mass of the coal *as received*, and M_{dry} is the mass of the dry coal.

Separation of Combustion Phases

In the present paper, we have used three variables to separate combustion phases (temperature, visible smoke and CO), by observation and data interpretation. During the ignition phase, there was noticeable white to brown smoke, characterised by an increase in CO emissions (4500 ppm) and low temperature (< 200°C). During the flaming stage, the temperature increased to above 400°C, while the CO emissions decreased (~1500 ppm) and there was a significant flame protruding from the top of the stove. During the coking phase, the CO emissions (900 ppm) and temperature (~300°C) are relatively stable, with no visible flame. At this stage, the combustion conditions are homogeneous and only coke/fixed carbon is burning, and heat transfer is in the form of radiant heat. A full description of the separation of the combustion phases in coal-burning braziers is presented in Makonese *et al.* (2015).

Particle Measurement

The sampling platform for monitoring PM was located at a distance of 2.5 m from the combustion hut, in a data capturing room, where all particle and gaseous measuring instruments are stationed. Fig. 2 shows a schematic presentation of the measurement and sampling system.

First, a sample of the exhaust was drawn from the chimney and diluted using the SeTAR variable dilution system. The SeTAR Centre dilution system was used to dilute the exhaust to protect the NanoScan Scanning Mobility Particle Sizer from clogging. Burning coal using braziers produce high levels of emissions, especially during ignition and flaming. It is essential to dilute the particles concentration to below the upper limit of detection of 1E6 # cm^{-3}. The dilution air is pre-heated by residual heat from combustion; this will not lead to modification of particles through either

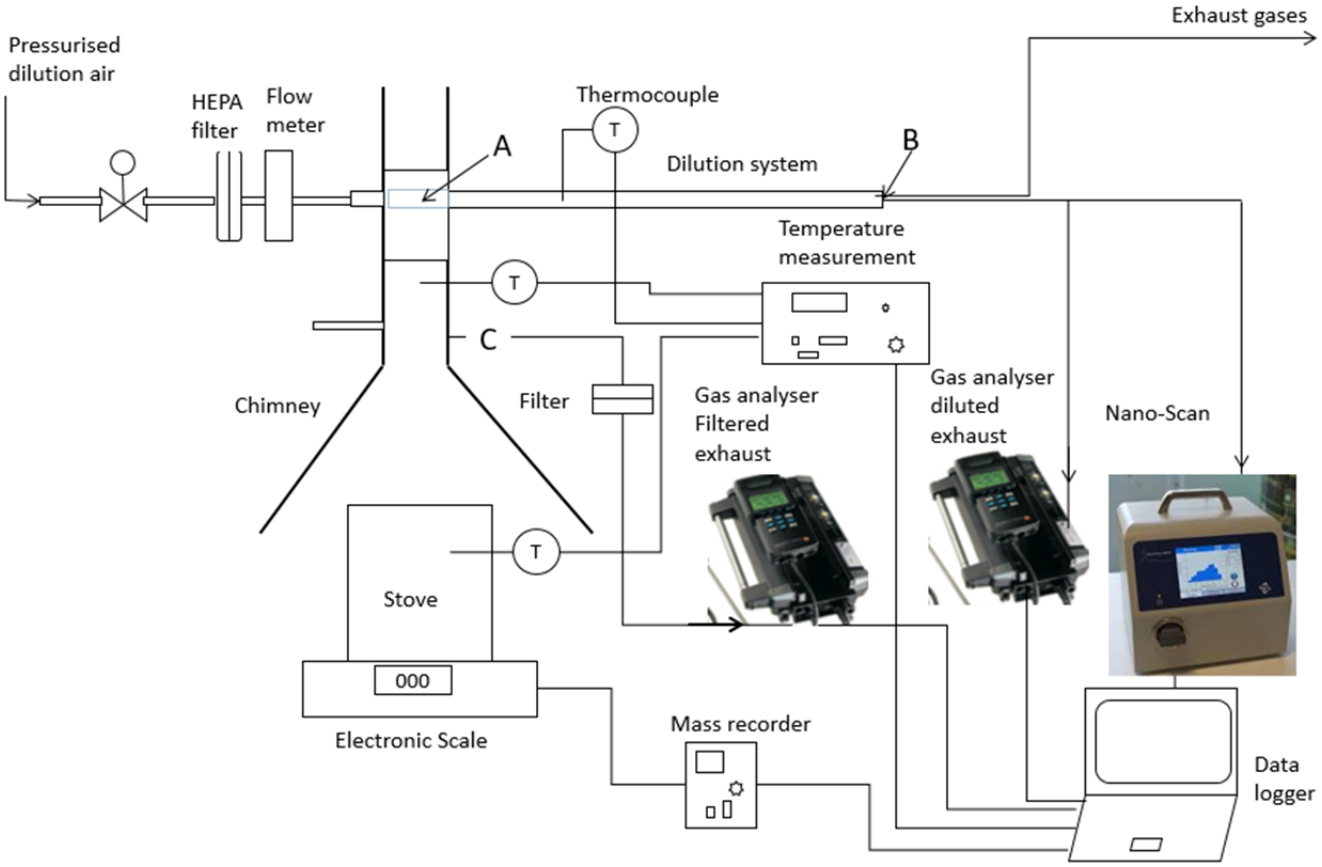

Fig. 2. Schematic diagram of the SeTAR Centre testing rig.

condensation or coagulation in dilution channel. The diluted sample was directed to a NanoScan Scanning Mobility Particle Sizer (SMPS) and a Testo XL 350 flue gas analyzer. The NanoScan Scanning Mobility Particle Sizer 3910 (TSI Inc., Shoreview, MN, USA) was used to study particles with a diameter ranging between 10 nm and 420 nm. The instrument response time is 3 seconds but averages size distribution over a 60 second interval (45 s upscan, 15 s downscan). The instrument measures particles continuously and records a maximum of 1E+06 particles cm^{-3}.

The undiluted sample was channelled to a Testo XL 350 flue gas analyser (Testo Inc., Sparta, USA). The Testo gas analyser is coupled with sensors that measures CO_2, CO, NO_x, NO_2, H_2, H_2S, S, SO_2 and O_2. The monitor is equipped with measurement modules for O_2, CO, NO and NO_2 as standard. Also, measurement modules for C_XH_Y, NO_{low}, $COlo_w$, SO_2, H_2S or CO_2 by the infrared are optionally available. The monitor uses electrochemical cells for gas measurements. CO_2 is determined using a non-dispersive infrared cell and is typically depicted as CO_2 IR. Oxygen balance is used for the calculation of excess air.

The design of the sampling system enabled the carbon dioxide mixing ratios of the diluted and undiluted exhaust to be measured to determine the dilution ratio, using the method described in Makonese (2015). Instantaneous dilution levels across the entire burn sequence were multiplied with the instantaneous particle concentrations to convert the diluted concentrations to undiluted exhaust concentrations (Eq. (2)).

$$DR = \frac{CO_{2(i)undiluted} - CO_{2ambient}}{CO_{2(i)diluted} - CO_{2ambient}} \quad (2)$$

where $CO_{2(i)undiluted}$ is the percentage of carbon dioxide in a raw sample; CO_2 is the ambient carbon dioxide concentration measured, and $CO_{2(i)}$ is the percentage of carbon dioxide in a diluted sample. Makonese (2015) reports further details of the SeTAR Centre dilution system in a study that systematically investigated smoke emissions from domestic coal combustion devices.

Quality Control

Before sampling, the dilution system was assembled, cleaned using potable water to remove any particles and other residual materials. After that, the dilution system was re-assembled, compressed air was blown in, and leaks were checked. Both the SMPS and Testo instruments are sent for calibration and servicing according to the manufacturer's recommendations, or at least once per annum, and are also periodically verified with laboratory standards. Zero and span calibration were performed on all analyzers before and after every test run to account for small variations in the dilution ratio. For example, the NanoScan was zeroed with filtered air before each test run. Tests were repeated three or more times to check for repeatability, due to the

heterogeneous nature of coal. The same person did the fire preparation to minimize variability in setting up, which might alter the combustion performance. We further subdivided the burn cycle into three combustion phases (i.e., ignition, flaming and coking). The tests were run for equal durations of three hours, and the combustion phases were separated for the three tests. Each combustion phase was further split into two stages, early and late. The test results were averaged over the three definitive tests.

Background concentrations were accounted for because particles from outside the testing facility can infiltrate the testing laboratory and contribute to the final concentration reading. In addition, other internal activities or airflow might re-suspend particles, which could affect the results. This study employed the ARIMA model to remove the contribution of background concentration to the actual activity generating submicron particles (Klein *et al.*, 2011) (Eq. (3)). The instruments were run for an hour before the three-hour testing duration and after that operated on compressed air for 10 minutes, to remove any fugitive emissions along the sampling train.

$$C_{combustion} = C_{activity} - C_{without} \quad (3)$$

where the $C_{combustion}$ is the final concentration, $C_{activity}$ is the actual sample collected after the PM generating activity was taking place + background concentration. $C_{without}$ is the concentration of particles obtained in the absence of the activity under investigation.

Study Limitations

The study is limited to submicron particle size diameters of 10–365 nm emitted from freshly produced coal smoke in a high air ventilation brazier, ignited using TLUD. The high air ventilation brazier and the TLUD ignition method are currently advocated as significant performance optimization parameters in fixed-bed coal combustion in braziers; hence the tests were only limited to these two variables.

RESULTS AND DISCUSSION

The experiments described earlier enable us to generate information on the particle number concentrations and size distributions corresponding to combustion phases over the entire burn sequence. In Table 2, results of the fuel analysis carried out by the SANAS accredited external laboratory are presented. The fuel composition is essential to determining the combustion emissions. The particle size distribution is influenced by several factors, including the fuel properties, testing conditions, and measuring instrument (Hosseini *et al.*, 2010). In a separate study conducted by Chakrabarty *et al.* (2006), it was found that fuel with a high moisture content (wet) produced particles with a larger diameter relative to dry fuel combusted under the same conditions. In the study conducted by Makonese (2015), it was reported that high moisture content in fuel can improve or impair combustion. Combusting fuel with a high moisture content led to increased emissions of CO. Furthermore, the same study indicated that fuel with a high calorific value emitted high concentrations of CO and PM in poorly ventilated stoves, whereas the same fuel in highly ventilated stoves emitted reduced concentrations of CO and PM. Therefore, in order to reduce the uncertainty in reported PM size distributions, fuel analysis must be incorporated.

The results presented in Table 3 indicate that particles were emitted throughout the experiments. However, the

Table 2. Fuel analysis specification.

Parameter (Air Dried Basis)	Standard Method	Slater Mine D-Grade Coal
Moisture content (%)	ISO 5925	1.8
Volatiles (%)	ISO 562	20.3
Ash (%)	ISO 1171	24.2
Fixed carbon (%)	By difference	52.0
Calorific value (MJ kg^{-1})	ISO 1928	23.4
Calorific value (Kcal kg^{-1})	ISO 1928	5590
Total sulphur (%)	ASTM D4239	0.63
Carbon (%)	ASTM D5373	62.6
Hydrogen (%)	ASTM D5373	2.76
Nitrogen (%)	ASTM D5373	1.0
Oxygen (%)	By difference	5.0
Total silica as SiO_2 (%)	ASTM D4326	58.6
Aluminium as Al_2O_3 (%)	ASTM D4326	27.6
Total iron as Fe_2O_3 (%)	ASTM D4326	6.63
Titanium as TiO_2 (%)	ASTM D4326	0.82
Phosphorous as P_2O_5 (%)	ASTM D4326	0.55
Calcium as CaO (%)	ASTM D4326	2.30
Magnesium as MgO (%)	ASTM D4326	0.83
Sodium as Na_2O (%)	ASTM D4326	0.42
Potassium as K_2O (%)	ASTM D4326	0.79
Sulphur as SO_3 (%)	ASTM D4326	1.10
Manganese as MnO_2 (%)	ASTM D4326	0.12

Table 3. Particle number concentration per combustion phase relative to the entire burn sequence.

Phase	(# cm^{-3}) N = 3	Duration (minutes)	GMD (nm)	GSD (nm)
Entire Combustion Sequence	1,20E+07 (100%)	180	51.9	2.1
Ignition	2,71E+03 (0.02%)	20	109.8	18.4
Flaming	6,67E+06 (55%)	60	54.9	5.9
Coking	5,34E+06 (44%)	100	34.3	5,1

most particles were emitted during the flaming phase, followed by the coking phase, with the fewest particles emitted during the ignition phase.

By contrast, in studies conducted by Makonese *et al.* (2014) and Masekameni (2015), it was found that the most particles were emitted during the ignition phase, followed by the flaming and the coking phases. The difference between the current study and previous studies on this subject is the use of different units in reporting data, i.e., both Makonese and Masekameni's studies focused on the particle size diameter in the range of $PM_{2.5}$ to PM_{10}. The limitation of our study is that it focuses on submicron particles (11–365 nm) and does not attempt to cover the entire size range (11 nm–10 μm). However, other studies using different methods reported similar findings to our studies, when using particle diameter and mass. In a recent study conducted by Chu *et al.* (2017) simulating particle size distribution using the fractal theory and Monte Carlo technique found that the smaller particles were most dominant compared to larger particles.

Table 4 presents percentage shares of nucleation, Aitken, and accumulation modes at each combustion phase. The Aitken and the accumulation modes dominate the particle concentration during the ignition phase. At this phase, there is a limited supply of combustion air and low temperatures. The particles condense and coagulate to form larger particles. The flaming and coking phases are dominated by the nucleation mode, with a relatively small contribution in the accumulation mode. Particularly during the coking phase, the combustion conditions are favourable, with sufficient supply of oxygen. The volatile organic compounds are often driven out during flaming before the transition to the coking phase. During coking phase, only fixed carbon burns and the rate of combustion is limited by oxygen adsorption onto the carbon matrix. These results are reasonably comparable to Tiwari *et al.* (2014, 2015), where coal combustion particles were dominated by nucleation (47.2%) and Aitken (41.3%) modes. According to Chang *et al.* (2004), coal combustion particles are often in the range of 40–50 nm. Our study results agree with Chang *et al.* (2004)—most of the particles were reported to be in nucleation mode, especially during coking and flaming. The difference between our study and Tiwari *et al.* (2014) and Chang *et al.* (2004) are that our results are presented per combustion phase, while the results from the two studies are given over the entire combustion sequence. Tiwari *et al.* (2015) further studied particle mass accumulation using three size fractions (respirable, fine and ultrafine). In the same study it was found that accumulated mass of particle > 100 nm was 1.5 μg m^{-3} while particle in the range of > 100 nm but < 300 nm was 1 μg m^{-3}. Although in the present study size distribution is based on number concentration, the study agrees with Tiwari *et al.* (2015). In our study we found that particles were largely emitted during the flaming and coking phase where combustion conditions are likely to be favourable. Given that smaller particles occupy less mass but larger surface area, the results are comparable.

Before ignition, ambient particulate matter size distribution and number concentration were monitored to account for ambient PM contributions. Fig. 3 shows the number size distribution for the background PM measured using the TSI NanoScan Scanning Mobility Particle Sizer. Results showed a polydispersed size distribution, and the background particle concentrations decreased sharply above 180 nm. This result is similar to findings by Hosseini *et al.* (2010) who noted that background particle concentration decreases significantly above 200 nm. As expected, the background concentrations are lower than combustion-specific concentrations measured during the different phases of the burn sequence (Figs. 4–10).

In this study, an attempt was made to separate particle emissions over the different combustion phases during each burn sequence, using the criteria presented in Makonese *et al.* (2015). Details of this segregation are also described in detail in Makonese (2015). Fig. 4 shows a size distribution and number concentration for the ignition phase. During this phase, combustion conditions are smouldering, with limited oxygen supply and low flame temperatures. Particles emitted during this phase are often expected to be larger relative to particles emitted during the flaming and the coking phase because of incomplete combustion conditions. However, the number of particles emitted at this phase is lower compared to the other stages. The particles at this phase are more in the range of 64 nm to 365 nm. These results confirm the association between oxygen starved combustion with increasing emissions of

Table 4. Contribution of combustion phase on PSD for the three modes (Nucleation, Aitken and Accumulation).

Combustion phase	Nuclei (Dp < 50 nm) (%)	Aitken (Dp 50–100 nm) (%)	Accumulation (Dp > 100 nm) (%)
Ignition	15,3	45,5	39,2
Flaming	46,8	30,8	22,4
Coking	83,9	13,4	2,6

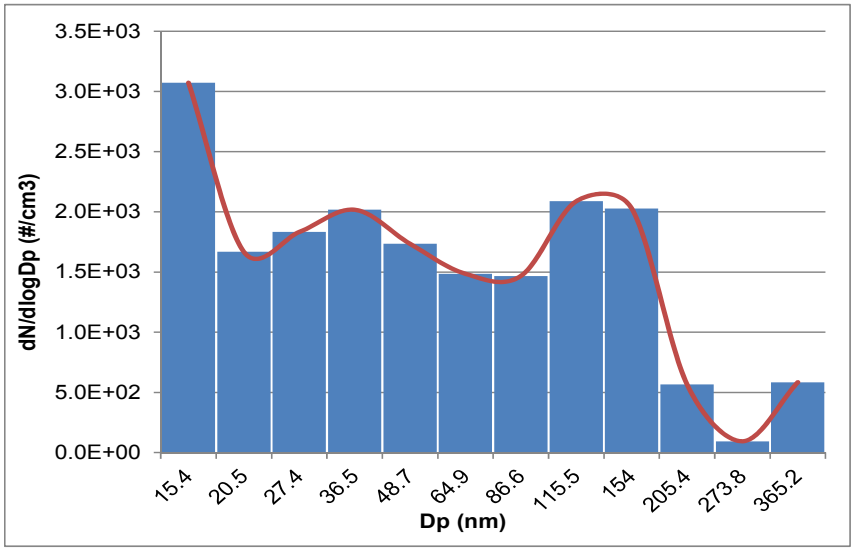

Fig. 3. Particle size distributions corresponding to the background concentrations.

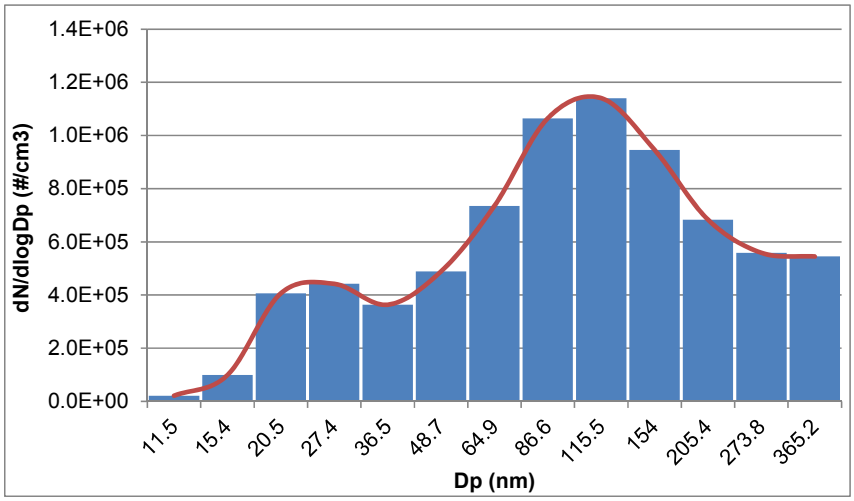

Fig. 4. Particle size distribution corresponding to the ignition phase.

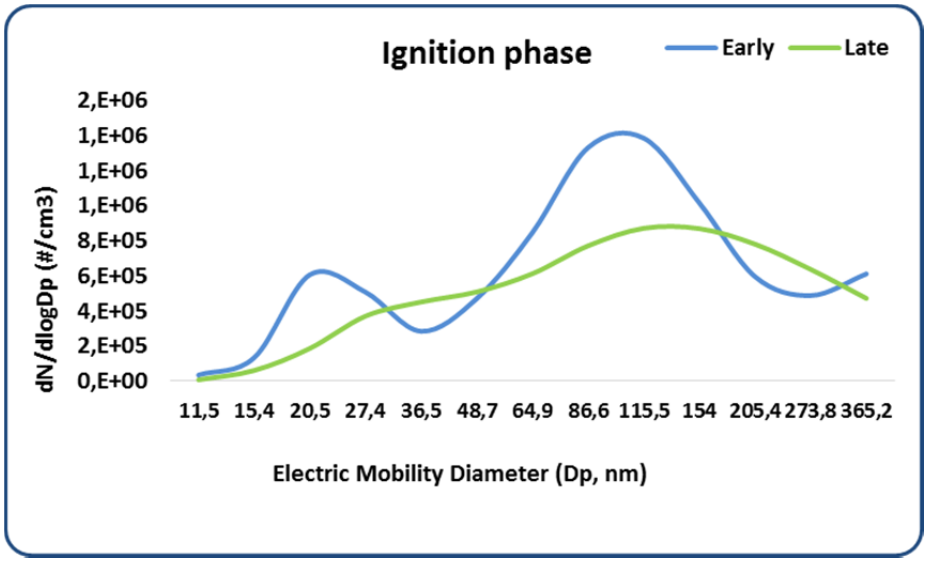

Fig. 5. Particle size distribution during early and late ignition.

larger particles. The ignition phase shows a bimodal distribution with a geometric mean diameter (GMD) of 109.8 ± 16.4 nm and a mode that is estimated at 145.3 nm.

The ignition phase was further divided into the early ignition (i.e., first 10 minutes) and late ignition (i.e., last 10 minutes of ignition)—the ignition phase constituted 20 minutes of the entire burning duration. Fig. 5 shows a bimodal size distribution during the early stages of combustion, with particle diameter at 109.8 ± 16.4 nm, while the mode diameter was estimated at 155.1 nm. Late ignition showed a near bimodal distribution with the particle mean diameter at 110.7 ± 20.6 nm, while the mode was determined at 134.6 nm. Early ignition will comprise mainly particles emitted from wood kindling, while the late ignition includes emissions from both wood kindling and coal. The mode diameter is greater during the early stage of ignition where smouldering conditions are imminent. However, the particle mean diameter was found to be similar. This finding suggests that there is no significant difference in particle diameter between the early and late ignition phases.

The bulk of particles emitted during a top-lit updraft coal fire were given off during the flaming stage (Fig. 6). The flaming phase showed a bimodal distribution with the GMD estimated at 54.9 ± 5.9 nm and the mode at 34.8 nm. Relative to ignition, number size distribution is reduced by 50%, which suggests that with improved combustion conditions more fine particles are emitted.

The number size distribution of particles during this flaming phase is similar to that of the average of the entire burn sequence (Fig. 6). Hosseini *et al.* (2010) reported similar findings when burning biomass under laboratory-controlled conditions. However, field measurements conducted by Zhang *et al.* (2015) reported a unimodal particle size distribution ranging from 70.3 to 75.7 nm. Furthermore, findings from the two studies, which are varied, might have been influenced by different testing conditions, i.e., field (uncontrolled) and laboratory (controlled). Also, sampling location regarding distance from the emitting source (Zhang *et al.*, 2015) and residence time, which might allow particle coagulation or agglomeration, could be an essential factor in this regard. Results from this study are comparable with previous limited studies, which attempted to study particle size distribution from domestic coal burning (McElroy *et al.*, 1982; Bond *et al.*, 2002; Hosseini *et al.*, 2010; Zhang *et al.*, 2012; Tiwari *et al.*, 2014).

The flaming phase was separated into early and late stages to differentiate number size distribution relative to improved combustion conditions. Fig. 7 shows a bimodal distribution during early flaming with a mode diameter at 39.8 nm while the mean diameter was at 67.6 ± 6.5 nm. Late flaming shows a near bimodal distribution with the mode diameter of 29.9 nm and the geometric mean diameter of 42.9 ± 5.5 nm. Particle GMD and mode diameter decreased by 36% and 25%, respectively, during late flaming relative to the early flaming phase. A decrease in mode diameter during this phase suggests improved combustion conditions, and particle diameter decreases with optimum combustion conditions.

During the coking phase, there were no visible flames, and the burning coal had turned into hot ambers. The period between the flaming phase and the coking phase referred to as the "mixed" phase in Hosseini *et al.* (2010) was not separately investigated in our study. However, Hosseini *et al.* (2010), separated particle distribution at the flaming phase; particle number concentration and number size distribution were reported at the start of flaming and for the mixed phase. For this study, the flaming and the "mixed" phases were collectively used under a single umbrella term "flaming phase", since the flame is still visible during the "mixed" phase.

The distribution during the coking phase showed a near unimodal particle size distribution with a GMD of 32.8 ± 5.1 nm and a mode of 31 nm (Fig. 8). The size distribution indicates that particle number concentration gradually increases above 180 nm. Particle number concentration during this phase is comparable to particle number concentrations during the flaming phase. A possible explanation for this is that during the coking phase (at the top of the fuel bed) there will be some coal still igniting and pyrolyzing at the bottom of the fuel bed. As the

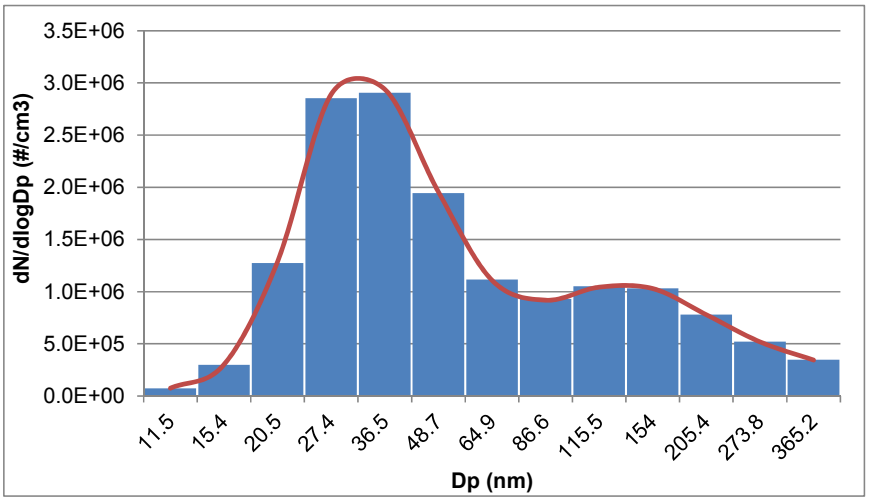

Fig. 6. Particle size distribution corresponding to the flaming phase.

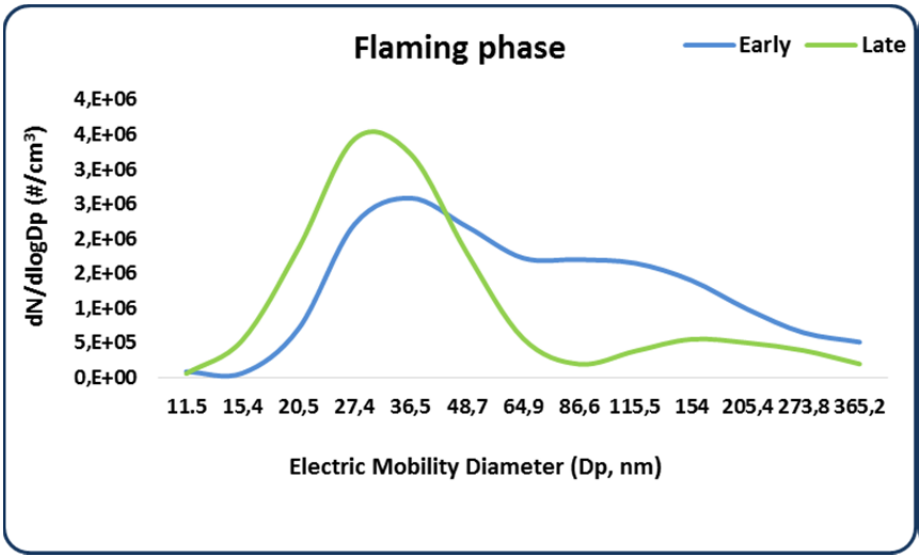

Fig. 7. Particle size distribution during early and late flaming.

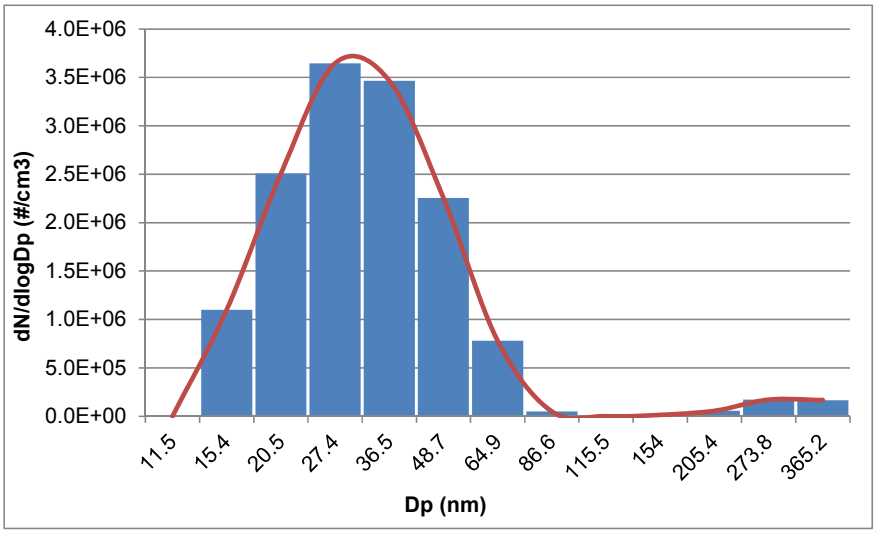

Fig. 8. Particle size distribution corresponding to the coking phase.

particles pass through the burning red-hot combustion zone, they are burned resulting in the emission of particles with a lower GMD. The results presented under this phase are similar to the one presented by Li *et al.* (2017); however, the study focused on particle size distribution from a coal-fired power station. A unimodal distribution was found but the average particle size was above 10 µm.

In Fig. 9, the coking phase was separated into two stages (i.e., early and late coking). Separation of the combustion phase did not produce different number size distributions, with the distribution similar to the entire phase average as indicated in Fig. 8. This is because the combustion conditions at this stage are homogeneous, with no visible flame nor smoke. Heat produced is in the form of radiant heat, and all volatiles have been driven out at the end of the flaming phase, and only fixed carbon burns with oxygen adsorption and temperature limiting the rate of combustion.

In Fig. 10, number size distribution and particle number concentration corresponding to the entire burn sequence are presented. The average number size distribution for the whole combustion sequence was found to be nearly bimodal, with a particle mode of 130 nm. After this mode, above 180 nm, particle number concentration was reduced gradually, and the GMD and mode were determined to be 51.6 ± 2.0 nm and 50.6 nm, respectively.

Other studies also showed PSD from all combustion phases to be bimodal with particle concentrations peaking between 30 and 150 nm (Hays *et al.*, 2002; Hedberg *et al.*, 2002; Hosseini *et al.*, 2010; Zhang *et al.*, 2011; Zhang *et al.*, 2012). Bond *et al.* (2002) observed that burning coal briquettes particles are emitted in size range between 20 and 100 nm. Earlier lab-based studies have found bimodal PSD from pulverized coal combustion with fine particle mode peaking at around 100 nm (McElroy *et al.*, 1982).

Based on the results given in the figures above, where combustion phases were separated, and size distribution

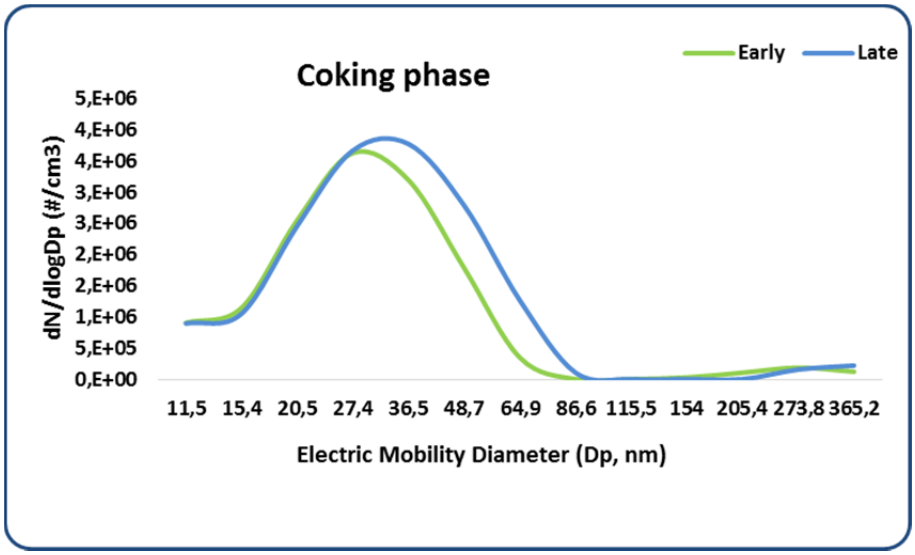

Fig .9. Particle size distribution during early and late coking.

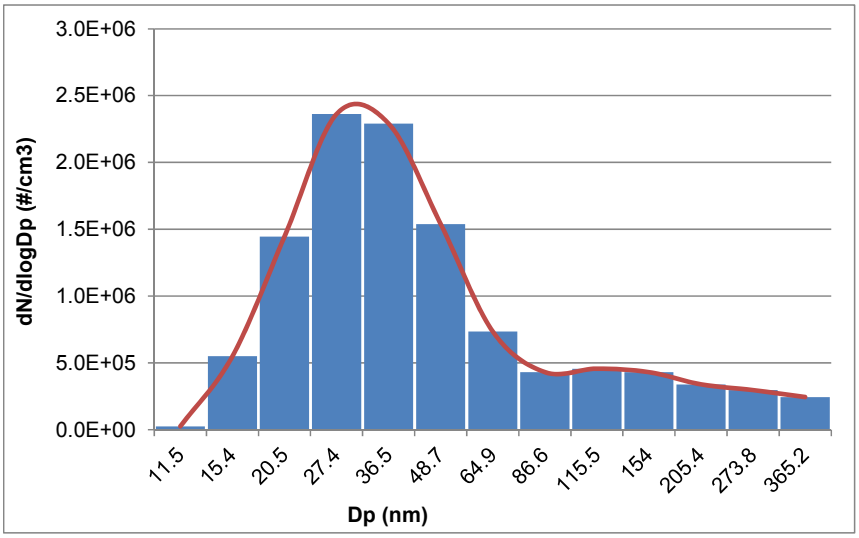

Fig .10. Particle size distribution corresponding to the entire burn cycle.

have been reported at each stage offers a meaningful insight on this subject (Fig. 10). Since the combustion conditions are not constant throughout the whole burn-sequence, it is essential to indicate number size distribution for each identical burn sequence. Looking at Fig. 10 only, one concludes that emissions of particles above 80 nm are attributable to the entire burn sequence. While the contribution of larger particles is associated with the ignition and early transitional combustion stage (i.e., ignition to early flaming) phase (Figs. 4–6), smaller particles are associated with both flaming and coking phases (Figs. 7–9). The ignition phase produced particles in the accumulation mode, which was influenced by smouldering conditions and the release of volatile organic compounds under low-temperatures. As the combustion progressed, there was a shift in particle mode from accumulation to Aitken, where particle diameter reduced during the transitional stage. During late flaming to coking, the mode changed to nucleation, where particle diameter further decreased under stable combustion conditions. This observation is similar to the distribution reported in Zhang *et al.* (2012).

SUMMARY AND CONCLUSION

This paper presents the number size distribution of the submicron particle fraction from combusting D-grade coal in a high air ventilation brazier using the top-lit updraft method. Particle size distributions were measured using a TSI NanoScan Scanning Mobility Particle Sizer. The monitor measured the PSD throughout the entire burn sequence (from ignition to coking). The PSD curves were separated into three combustion phases: ignition, flaming, and coking. The GMD of the particle size distribution was estimated to be 51.6 nm for the averaged burn sequence. Particle number concentrations were high during the flaming and coking phases compared to the ignition phase.

The GMD rapidly increased during the ignition phase and gradually decreased during the flaming and coking phases. The particle size distribution was bimodal across the first two combustion phases for the D-grade coal used in our experiments but was unimodal during the coking phase. The unimodal distribution suggests homogeneous combustion conditions, when the radiant heat flow is constant and the particle emissions are identical. All volatiles are driven out during the coking phase, with only fixed carbon burning under ideal combustion conditions and with a sufficient air supply. Although the study does not attempt to investigate the particle emission composition, we can anticipate that particle emission during the coking phase is attributable to fly ash. Despite limitations due to assessing the particle size distribution only for small-scale coal combustion, we have drawn lessons from other studies that focused on wood burning technologies. Studies conducted by multiple researchers reported a unimodal particle size distribution under ideal wood burning conditions (Hays *et al.*, 2002; Hedberg *et al.*, 2002; Hosseini *et al.*, 2010; Zhang *et al.*, 2011; Zhang *et al.*, 2012), while McElroy *et al.* (1982) reported a bimodal PSD. Nevertheless, in all of these studies, a bimodal distribution was attributed to poor combustion conditions and the agglomeration process.

We have demonstrated in this study that improving combustion conditions emits particles with a smaller diameter. This finding is worrying, given the consequences, as outlined in epidemiological studies, that smaller particles are easily inhaled and have a higher potential for uptake through blood circulation. However, the toxicity of these particles must be investigated for various combustion phases in order to draw conclusions regarding the potential health effects of emitted particles with varied number size distributions.

ACKNOWLEDGEMENTS

This work was supported financially by the University of Johannesburg through a URC fellowship grant to TM, and in part from a grant from the Global Alliance for Clean Cookstoves (GACC) to the SeTAR Centre as a Regional Stove Testing and Development Centre. The authors thank the National Institute for Occupational Health through Joel Maseki and Kevin Kasangana for assistance with the TSI NanoScan SMPS. Extended appreciation to Nomsa Thabethe for her contribution proofreading and editing of the manuscript.

REFERENCES

Anastasio, C. and Martin, S.T. (2001). Atmospheric nanoparticles. In *Nanoparticles and the environment*, Banfield, J.F. and Navrotsky, A. (Eds.), Mineralogical Society of America, Washington, DC, USA, pp. 293–349.

Andreae, M.O. and Merlet, P. (2001). Emission of trace gases and aerosols from biomass. *Global Biogeochem. Cycles* 15: 955–966.

Annegarn, H.J. and Sithole, J. (1997). Soweto air monitoring-project SAM, Annual report for the period January-December 1996, Department of Environment and Tourism, Report No. AER97.094-SAM, University of Witwatersrand, Johannesburg, South Africa.

Balmer, M. (2007). Household coal use in an urban township in South Africa. *JESA* 18: 27–32.

Barnes, B., Mathee, A. and Moiloa, K. (2005). Assessing child time – activity patterns in relation to indoor cooking fires in developing countries: A methodological comparison. *Int. J. Hyg. Environ. Health* 208: 219–225.

Barnes, B., Mathee, A., Thomas, E. and Bruce, A. (2009). Household energy, indoor air pollution and child respiratory health in South Africa. *JESA* 20: 4–13.

Bølling, A.K., Pagels, J., Yttri, K.E., Barregard, L., Sallsten, G., Schwarze, P.E. and Boman, C. (2009). Health effects of residential wood smoke particles: The importance of combustion conditions and physicochemical particle properties. *Part. Fibre Toxicol.* 6: 29.

Bond, T.C., Covert, D.S., Kramlich, J.C., Larson, T.V. and Charlson, R.J. (2002). Primary particle emissions from residential coal burning: Optical properties and size distributions. *J. Geophys. Res*. 107: 8347.

Bonjour, S., Adair-Rohani, H., Wolf, J., Bruce, N.G., Mehta, S., Prüss-Ustün, A., Lahiff, M., Rehfuess, E.A., Mishra, V. and Smith, K.R. (2013). Solid-fuel Use for Household Cooking: Country and Regional Estimates for 1980–2010. *Environ. Health Perspect*. 121: 784–790.

Bruce, N., Perez-Padilla, R and Albalak R. (2000). Indoor air pollution in developing countries: A major environmental and public health challenge. *Bull. World Health Organ.* 78: 1078–1092.

Chakrabarty, R.K., Moosmuller, H., Garro, M.A., Arnott, W.P., Walker, J., Susott, R.A., Babbitt, R.E., Wold, C.E., Lincoln, E.N., and Hao, W.M. (2006). Emissions from the laboratory combustion of wildland fuels: Particle morphology and size. *J. Geophys. Res*. 111: D07204.

Chakrabarty, R.K., Moosmüller, H., Garro, M.A. and Stipe, C.B. (2012). Observation of super-aggregates from a reversed gravity low-sooting flame. *Aerosol Sci. Technol.* 46: i–iii.

Chang, M.C.O., Chow, J.C., Watson, J.G., Hopke, P.K., Yi, S.M. and England, G.C. (2004). Measurement of ultrafine particle size distributions from coal-, oil-, and gas-fired stationary combustion sources. *J Air Waste Manage. Assoc*. 54: 1494–1505.

Chu, H., Zheng, Z., Ren, F. and Mingyan, G. (2017). Study on granularity distribution of powder by fractal models, *Fractals* 25: 1–6.

Cincinelli, A. and Martellini, T. (2017). Indoor air quality and health. *Int. J. Environ. Res. Public Health* 14: 1286.

CSIR (2005). Laboratory controlled quantitative information about reduction in air pollution using the "Basa *njengo* Magogo" methodology and applicability to low-smoke fuels (Revised), Division of Water, Environment and Forestry Technology, CSIR Durban, Report No. ENV-D 2005.

Department of Minerals and Energy (DME) (2004). Integrated household clean energy strategy, Department of Minerals and Energy, Pretoria, South Africa.

Department of Minerals and Energy (DME) (2006). Digest of South African energy statistics 2003/2004, Directorate, Energy Planning and Development, Department of Minerals and Energy, Pretoria, South Africa.

Dockery, D.W., Pope, C.A., Xu, X., Spengler, J.D., Ware, J.H., Fay, M.E., Ferris, B.G. and Speizer, F.E. (1993). An association between air pollution and mortality in six U.S. cities. *N. Engl. J. Med.* 329: 1753–1759.

Ezzati, M and Kammen, D.M. (2001). Indoor air pollution from biomass combustion as a risk factor for acute respiratory infections in Kenya: An exposure-response study. *Lancet* 358: 619–624.

Fernandez, A., Wendt, J.O.L., Wolski, N., Hein, K.R.G., Wang, S. and Witten, M.L. (2003). Inhalation health effects of fine particles from the co-combustion of coal and refuse derived fuel. *Chemosphere* 51: 1129–1137.

Forouzanfar, M.H., Alexander, L., Anderson, H.R., Bachman, V.F., Biryukov, S., Brauer, M., Burnett, R., Casey, D., Coates, M.M., Cohen, A., *et al.* (2015). Global, regional, and national comparative risk assessment of 79 behavioural, environmental and occupational, and metabolic risks or clusters of risks in 188 countries, 1990-2013: A systematic analysis for the Global Burden of Disease Study 2013. *Lancet* 386: 2287–323.

Gladney, E.S. (1974). *Trace element emissions from coal-fired power plants: A study of the chalk point electric generating station*. Ph.D. Thesis, University of Maryland, USA.

Gladney, E.S. (1976). Composition and size distribution of in-stack particulate material at a coal-fired power plant. *Atmos. Environ*. 10: 1071–1077.

Global Alliance for Clean Cookstoves (GACC) (2009). GACC, http://cleancookstoves.org/2009.

Gordon, S.B., Bruce, N.G., Grigg, J., Hibberd, P.L., Kurmi, O.P., Lam, K.B., Mortimer, K., Asante, K.P., Balakrishnan, K., Balmes, J., Bar-Zeev, N., Bates, M.N., Breysse, P.N., Buist, S., Chen, Z., Havens, D., Jack, D., Jindal, S., Kan, H., Mehta, S., Moschovis, P., Naeher, L., Patel, A., Perez-Padilla, R., Pope, D., Rylance, J., Semple, S. and Martin, W.J., II (2014). Respiratory risks from household air pollution in low and middle-income countries. *Lancet Respir. Med.* 2: 823–860.

Hays, M.D., Geron, C.D., Linna, K.J., Dean Smith, N. and Schauer, J.J. (2002). Speciation of gas-phase and fine particle emissions from burning of foliar fuels. *Environ. Sci. Technol*. 36: 2281–2295.

Hedberg, E., Kristensson, A., Ohlsson, M., Johansson, C., Johansson, P., Swietlicki, E., Vesely, V., Wideqvist, U. and Westerholm, R. (2002). Chemical and physical characterization of emissions from birch wood combustion in a wood stove. *Atmos. Environ*. 36: 4823–4837.

Hosseini, S., Li, Q., Cocker, D., Weise, D., Miller, A., Shrivastava, M., Miller, J.W., Mahalingam, S., Princevac, M. and Jung, H. (2010). Particle size distributions from laboratory-scale biomass fires using fast response instruments. *Atmos. Chem. Phys*. 10: 8065–8076.

International Energy Agency (2015). World Energy Outlook, www.worldenergyoutlook.org.

ISO IWA 11:2012 (2012). Guidelines for Evaluating Cookstove Performance. http://cleancookstoves.org/resources_files/iso-iwa-cookstoves.pdf.

Jiang, R. and Bell, M.L. (2008). A comparison of particulate matter from biomass-burning rural and non-biomass-burning urban households in northeastern China. *Environ. Health Perspect.* 116: 907–914.

Kasangana, K.K., Masekameni, M.D. and Saliwa, S. (2017). Exploring access to clean energy for various domestic uses in Mpumalanga province, South Africa. Proceedings of the 26th Domestic Use of Energy (DUE) Conference, 4-5 April 2017, South Africa, Cape Town, South Africa, pp. 116–120.

Kauppinen E.I. and Pakkanen, T.O. (1990). Coal combustion aerosols: A field study. *Aerosol Sci. Technol*. 24: 1811–1818.

Kittelson, D.B. (1998). Engines and nanoparticles: A REVIEW. *J. Aerosol Sci.* 29: 575–588.

Klein, E.R.H., Fransman, W. and Brouwer, D.H. (2011). How to statistically analyze nano exposure measurement results: Using an ARIMA time series approach. *J. Nanopart. Res.* 13: 6991–7004.

Kumar, P., Gurjar, B.R., Nagpure, A. and Harrison, R.M. (2011). Preliminary estimates of nanoparticle number emissions from road vehicles in megacity Delhi and associated health impacts. *Environ. Sci. Technol*. 45: 5514–5521.

Kumar, P., Robins, A., Vardoulakis, S. and Britter, R. (2010). A review of the characteristics of nanoparticles in the urban atmosphere and the prospects for developing regulatory controls. *Atmos. Environ.* 44: 5035–5052.

Le Roux, L.J., Cilliers, K.F.P. and Van Vuuren, D.S. (2004). Low-smoke fuels standard testing and verification. Final Report to the Department of Minerals and Energy. CSIR Report No. 86DC / HT776.

Li, Z., Ji, Y., Ma, H., Zhao, P., Zeng, X., Liu, S., Jiang, Y., Wang, L., Liu, A., Gao, H., Liu, F. and Mwangi, J.K. (2017). Characterization of inorganic elements within $PM_{2.5}$ and PM_{10} fractions of fly ashes from coal-fired power plants. *Aerosol Air Qual. Res*. 17: 1105–1116.

Lim, S.S., Vos, T., Flaxman, A.D., Danaei, G., Shibuya, K. and Adair-Rohani, H. (2012). A comparative risk assessment of burden of disease and injury attributable to 67 risk factors and risk factor clusters in 21 regions, 1990–2010: A systematic analysis for the Global Burden of Disease Study 2010. *Lancet* 380: 2224–2260.

Linak, W.P., Miller, C.A., Seames, W.S., Wendt, J.O.L., Ishinomori, T., Endo, Y. and Miyamae, S. (2002). On trimodal particle size distributions in fly ash from pulverized-coal combustion. *Proc. Combust. Inst.* 29: 441–447.

Makonese, T. (2015). *Systematic investigation of smoke emissions from packed-bed residential coal combustion devices*, PhD Thesis, University of Johannesburg, South Africa.

Makonese, T., Forbes, P., Mudau, L. and Annegarn, H. (2014). Aerosol particle morphology of residential coal combustion. *Clean Air J.* 24: 24–28.

Makonese, T., Masekameni, D., Forbes, P. and Annegarn,

H. (2015). Influence of fire-ignition methods and air ventilation rates on the gaseous and condensed matter (smoke) emissions from residential coal-burning braziers. *JESA* 26: 16–28.

Masekameni, M.D. (2015). *Performance evaluation and emission characterization of domestic coal combustion in optimized braziers*. MSc thesis, University of Johannesburg South Africa.

Masekameni, M.D., Makonese, T. and Annegarn, H.J. (2014). Optimisation of ventilation and ignition method for reducing emissions from coal-burning imbaulas. Proceedings of the 22nd Domestic Use of Energy (DUE) Conference, 30 March–2 April 2014, IEEE Conference Publications, Cape Town, South Africa.

McElroy M.W., Carr R.C., Ensor D.S. and Markowski G.R. (1982). Size distribution of fine particles from coal combustion. *Science* 215: 13–19.

Morawska, L., Ristovski, Z., Jayaratne, E.R., Keogh, D.U. and Ling, X. (2008). Ambient nano and ultrafine particles from motor vehicle emissions: Characteristics, ambient processing and implications on human exposure. *Atmos. Environ*. 42: 8113–8138.

Naeher, L.P., Brauer, M., Lipsett, M., Zelikoff, J.T., Simpson, C.D., Koenig, J.Q. and Smith, K.R. (2007). Woodsmoke health effects: A review. *Inhalation Toxicol.* 19: 67–106.

Oberdörster, G., Sharp, Z., Atudorei, V., Elder, A., Gelein, R., Kreyling, W. and Cox, C. (2004). Translocation of inhaled ultrafine particles to the brain. *Inhalation Toxicol.* 16: 437–445.

Oberdörster, G., Oberdörster, E. and Oberdörster, J. (2005). Nanotoxicology: An Emerging discipline evolving from studies. *Environ. Health Perspect.* 113: 823–829.

Rainey, K.L., Vaganay, M. and MacIntyre, S. (2016). A review of literature on residential solid-fuel burning, and consequently the implications of meeting the European 2050 low-carbon targets. *J. Geosci. Environ. Prot.* 4: 7–13.

Scorgie, Y. (2012). *Urban air quality management and planning*, PhD thesis University of Johannesburg, South Africa.

Scorgie, Y., Kneen, M.A., Burger, L.W. and Annegarn, H.J. (2003). Air pollution in the Vaal Triangle - quantifying, source contributions and identifying cost effective solutions. Proceedings of the 11th National Association for Clean Air Conference.

Shonkoff, S.B., Krewski, D, Pope, C.A. III, Thun, M.J. and Thurston, G. (2009). Public health benefits of strategies to reduce greenhouse-gas emissions: health implications of short-lived greenhouse pollutants. *Lancet* 374: 2091–2103.

Sioutas, C., Dolfino, R.J. and Singh, M. (2005). Exposure assessment for atmospheric ultrafine particles (UFPs) and implications in epidemiologic research. *Environ. Health Perspect.* 113: 947–955

Smith, K.R., Apte, M.G., Yuqing, M., Wongsekiarttirat, W. and Kulkarni, A. (1994). Air pollution and the energy ladder in Asian cities. *Energy* 19: 587–600.

Smith, K.R., Mehta, S. and Maeusezahl-Feuz, M. (2004). Comparative quantification of health risks: Global and regional burden of disease attributable to selected major risk factors, Ezzati, M., Rodgers, A.D., Lopez, A.D. and Murray, C.J.L. (Eds,), World Health Organization, Geneva, pp. 1435–1493.

Smith, K.R., Dutta, K., Chengappa, C., Gusain, P.P.S., Berrueta, O.M., Victor, Edwards, R., Bailis, R. and Shields, K.N. (2007). Monitoring and evaluation of improved biomass cookstove Programs for indoor air quality and stove performance: Conclusions from the Household Energy and Health Project. *Energy Sustainable Dev.* 11: 6–18.

Smith, K.R. and Peel, J.L. (2010). Mind the gap. *Environ. Health Perspect.* 118: 1643–1645.

Statistic South Africa (2001). *Causes of death in South Africa 1997-2001, advanced recorded causes of death*. Pretoria, South Africa.

Statistic South Africa (2001). *Census 2001, detailed demographic databases*. Pretoria, South Africa.

Stats SA (2010). Statistical release P0309.3. Mortality and causes of death in South Africa. http://www.statssa.gov.za

Terblanche, A.P., Opperman, L., Nel, C.M. and Nyikos, H. (1993). Exposure to air pollution from transitional household fuels in a South African population. *J. Exposure Anal. Environ. Epidemiol.* 3: 15–22.

Terblanche, P. and Pols, A.S. (1994). Characterisation of risk factors associated with household fuel usage in South Africa, Report compiled on behalf of Department of Minerals and Energy, Report No. EO 9303, July 1994, Pretoria, South Africa.

Tiwari, M., Sahu, S.K., Bhangare, C., Yousaf, A. and Pandi, G.G. (2014). Particle size distributions of ultrafine combustion aerosols generated from household fuels. *Atmos. Pollut. Res*. 5: 145–150.

Tiwari, M., Sahu, S.K. and Pandit, G.G. (2015). Inhalation risk assessment of PAH exposure due to combustion aerosols generated from household fuels. *Aerosol Air Qual. Res*. 15: 582–590.

Tranfield, E.M. and Walker, D.C. (2012). Understanding of human illness and death following exposure to particulate matter air pollution. In *Environmental health – Emerging issues and practice*, Oosthuizen, J. (Ed.), Intech, Rijeka, Croatia, pp. 81–102.

Van Niekerk, W.C.A., Britton, M.T.S. and Laurens, J.B. (1997). *Laboratory technical tests-determination of emission factors*. Department of Minerals and Energy, Pretoria, South Africa.

World Health Organization (2014). *WHO Guidelines for Indoor Air Quality: Household Fuel Combustion*. WHO Document Production Services, Geneva.

Xu, M., Yu, D., Yao, H., Liu, X. and Qiao, Y. (2011). Coal combustion-generated aerosols: Formation and properties. *Proc. Combust. Inst.* 33: 1681–1697.

Yi, H., Hao, J., Duan, L., Tang, X., Ning, P. and Li, X. (2008). Fine particle and trace element emissions from an anthracite coal-fired power plant equipped with a bag-house in China. *Fuel* 87: 2050–2057.

Zhang, H., Wang, S., Hao, J., Wan, L., Jiang, J., Zhang, M., Mestl, H.E.S., Alnes, L.W.H., Aunan, K. and Mellouki,

A.W. (2012). Chemical and size characterization of particles emitted from the burning of coal and wood in rural households in Guizhou, China. *Atmos. Environ*. 51: 94–99.

Zhang, H.F., Hu, D.W., Chen, J.M., Ye, X.N., Wang, S.X., Hao, J.M., Wang, L., Zhang, R.Y. and An, Z.S. (2011). Particle size distribution and polycyclic aromatic hydrocarbons emissions from agricultural crop residue burning. *Environ. Sci. Technol*. 45: 5477–5482.

Zhang, J.J. and Smith, K.R. (2007). Household Air Pollution from Coal and Biomass Fuels in China: Measurements, Health Impacts, and Interventions. *Environ. Health Perspect.* 115: 848–855.

Zhang, T.R., Wooster, M.J., Green, D.C. and Main, B. (2015). New field-based agricultural biomass burning trace gas, $PM_{2.5}$, and black carbon emission ratios and factors measured in situ at crop residue fires in Eastern China. *Atmos. Environ*. 121: 22–34.

Received for review, April 23, 2018
Revised, July 19, 2018
Accepted, July 27, 2018